
PROBABILITY DISTRIBUTION OF HYPERVOLUME IMPROVEMENT IN BI-OBJECTIVE BAYESIAN OPTIMIZATION

A PREPRINT

Hao Wang

Leiden University
Leiden, The Netherlands
h.wang@liacs.leidenuniv.nl

Kaifeng Yang*

University of Applied Sciences Upper Austria
Hagenberg, Austria
kaifeng.yang@fh-hagenberg.at

Michael Affenzeller

University of Applied Sciences Upper Austria
Hagenberg, Austria
michael.affenzeller@fh-hagenberg.at

Michael Emmerich

Leiden University
Leiden, The Netherlands
m.t.m.emmerich@liacs.leidenuniv.nl

ABSTRACT

This work provides the exact expression of the probability distribution of the hypervolume improvement (HVI) for bi-objective generalization of Bayesian optimization. Here, instead of a single-objective improvement, we consider the improvement of the hypervolume indicator concerning the current best approximation of the Pareto front. Gaussian process regression models are trained independently on both objective functions, resulting in a bi-variate separated Gaussian distribution serving as a predictive model for the vector-valued objective function. Some commonly HVI-based acquisition functions (probability of improvement and upper confidence bound) are also leveraged with the help of the exact distribution of HVI. In addition, we show the superior numerical accuracy and efficiency of the exact distribution compared to the commonly used approximation by Monte-Carlo sampling. Finally, we benchmark distribution-leveraged acquisition functions on the widely applied ZDT problem set, demonstrating a significant advantage of using the exact distribution of HVI in multi-objective Bayesian optimization.

1 Introduction

For solving multi-objective optimization problems (MOPs), the hypervolume indicator (HV) is extensively employed for assessing the quality of the Pareto front approximation. The HV is defined as the Lebesgue measure (in 2-D the area) of the dominated sub-space of \mathbb{R}^m by some approximation set A to the Pareto front. To make the measure finite, we bound the measured subspace from above by a reference point. Originally, the hypervolume indicator was proposed in the context of benchmarking multi-objective optimization algorithms (MOAs), and more recently, it has found broader application in various exact and stochastic optimization algorithms, e.g., for guiding the search in so-called indicator-based evolutionary algorithms [BNE07, DAP⁺02] and Bayesian optimization [EYD⁺16, YED⁺19b, EYD20, DBB20]. In this work, we target the Bayesian optimization (BO) algorithms for tackling the bi-objective optimization problems, in which a derivative of HV - the *hypervolume improvement* (HVI) that measures the increment of the HV value after adding new points to the Pareto front - often plays a vital role for defining the so-called *acquisition function*, which quantifies the “potential” of evaluating unseen points in the decision space. Loosely speaking, in the Bayesian setting, the objective function value that corresponds to an unseen point is modeled as a multivariate Gaussian random variable, which brings uncertainty to assessing the HVI value of this point. Several acquisition functions have been devised to incorporate such an uncertainty, e.g., the probability of improvement (PoI) [EGN06, Kea06] that computes the chance of realizing a strictly positive HVI, the naïve Upper Confidence Bound (naïve-UCB) [EYD20] that assesses the HVI value

*Corresponding author.

of an upper bound of the objective values, and the expected hypervolume improvement (EHVI) [EGN06, YED⁺19a] that evaluates the average HVI.

Despite the successful application of these acquisition functions, none of them considers the actual distribution of the hypervolume improvement, which can be essential when dealing with more challenging multi-modal MOPs. In this paper, we aim to provide the exact form of the probability distribution functions of the HVI for bi-objective MOPs and subsequently propose two novel acquisition functions which directly utilize the distribution of HVI. Also, we compare the numerical computation of the exact distribution to that of the Monte-Carlo (MC) method, which shows the superiority of the exact distribution over MC in terms of computation accuracy and time complexity. Lastly, we tested, on the well-known ZDT benchmark problems [ZDT⁺00], the new distribution-based acquisition functions against some commonly-used state-of-the-art alternatives, where we observed a significant improvement of BO's performance with the help of the new distribution-based acquisition functions over their counterparts.

This paper is organized as follows. Sec. 2 provides a concise recap of the background and related works. Sec. 3 elucidates in detail the derivation of the probability distribution of HVI. In Sec. 4, we propose two novel acquisition functions based on the distribution of HVI, followed by the experimental study thereof. In addition, we will denote by $\phi_{\mu,\sigma}$ and $\Phi_{\mu,\sigma}$ the PDF and CDF of a Gaussian random variable with mean μ and standard deviation σ , respectively.

2 Preliminaries

Multi-objective optimization A real-valued multi-objective optimization problem (MOP) involves minimizing multiple objective functions simultaneously, i.e., $\mathbf{f} = (f_1, \dots, f_m)$, $f_i : \mathcal{X} \rightarrow \mathbb{R}$, $\mathcal{X} \subseteq \mathbb{R}^d$, $i \in [1..m]$. For every $\mathbf{y}^{(1)}$ and $\mathbf{y}^{(2)} \in \mathbb{R}^m$, we say $\mathbf{y}^{(1)}$ weakly dominates $\mathbf{y}^{(2)}$ (written as $\mathbf{y}^{(1)} \preceq \mathbf{y}^{(2)}$) iff. $y_i^{(1)} \leq y_i^{(2)}$, $i \in [1..m]$. The Pareto order \prec on \mathbb{R}^m is defined: $\mathbf{y}^{(1)} \prec \mathbf{y}^{(2)}$ iff. $\mathbf{y}^{(1)} \preceq \mathbf{y}^{(2)}$ and $\mathbf{y}^{(1)} \neq \mathbf{y}^{(2)}$. A point $\mathbf{x} \in \mathcal{X}$ is efficient iff. $\nexists \mathbf{x}' \in \mathcal{X} (\mathbf{f}(\mathbf{x}') \prec \mathbf{f}(\mathbf{x}))$. The set of all efficient points of \mathcal{X} is called the *efficient set*. The image of the efficient set under \mathbf{f} is called the *Pareto front*. Multi-objective optimization algorithms (MOAs) often employ a finite multiset $X = \{\mathbf{x}^{(1)}, \dots, \mathbf{x}^{(n)}\}$ to approximate the efficient set, whose image under \mathbf{f} is denoted by Y . The *non-dominated subset* of Y is a finite approximation to the Pareto front, which is denoted by \mathcal{P} . *Non-dominated space* w.r.t. \mathcal{P} is the subset of \mathbb{R}^m that is not dominated by \mathcal{P} , i.e., $\text{ndom}(\mathcal{P}) := \{\mathbf{y} \in \mathbb{R}^m : \nexists \mathbf{p} \in \mathcal{P} (\mathbf{p} \prec \mathbf{y})\}$. Similarly, the *dominated space* w.r.t. \mathcal{P} is the complement of $\text{ndom}(\mathcal{P})$. Evolutionary algorithms are of particular interest for solving MOPs, e.g., NSGA-II [DAP⁺02] and SMS-EMOA [BNE07], which, however, suffer from a high sample complexity (see [YLD⁺16]). In this paper, we focus on the multi-objective Bayesian optimization (MOBO) [EYD⁺16] algorithms that utilize a probabilistic model of the objective function to achieve a lower sample complexity.

Bayesian Optimization BO [Moc74, JSW98, SSW⁺16] is a sequential model-based optimization algorithm which is originally proposed to solve the single-objective black-box optimization problems that are expensive to evaluate. BO starts with sampling a small initial design of experiment (DoE, obtained with e.g., Latin Hypercube Sampling) $X \subseteq \mathcal{X}$. After evaluating X with \mathbf{f} , it proceeds to construct a probabilistic model $\Pr(\mathbf{f} \mid X, Y)$ (e.g., Gaussian process regression). BO balances the exploration and exploitation of the search by considering, for a decision point \mathbf{x} , two information - the prediction $\hat{f}(\mathbf{x})$ and the uncertainty thereof. Both information are taken to define an acquisition function, e.g., the expected improvement, to quantify the potential of each point for making progresses. BO chooses the next point to evaluate by maximizing the acquisition function. The multi-objective generalization [YED⁺19b, YDY⁺16, YED⁺19a, YPE⁺19, EYD20, DBB20] has been proposed particularly based on the hypervolume improvement [EYD⁺16] as it can be generalized to the multi-objective counterpart of the expected improvement.

Gaussian process regression For modelling a vector-valued objective function, we take the most straightforward method, which models each objective function as the realization of a centered² Gaussian process (GP) prior [RW06], i.e., $\forall i \in [1..m]$, $f_i \sim \text{gp}(0, k_i)$, where $k_i : \mathcal{X} \times \mathcal{X} \rightarrow \mathbb{R}$ is a positive definite function (e.g., the Matérn kernel [Gen01]) that computes the auto-covariance of f_i , i.e., $\forall \mathbf{x}, \mathbf{x}' \in \mathcal{X}$, $k_i(\mathbf{x}, \mathbf{x}') = \text{Cov}\{f_i(\mathbf{x}), f_i(\mathbf{x}')\}$. Given a data set $\mathcal{D} = (X, Y)$ comprising n points $X = \{\mathbf{x}^{(1)}, \dots, \mathbf{x}^{(n)}\} \subset \mathcal{X}$ and their objective values $Y = \{\mathbf{f}(\mathbf{x}^{(1)}), \dots, \mathbf{f}(\mathbf{x}^{(n)})\}$, this method learns independent posterior GPs for each objective function, i.e., $f_i \mid \mathcal{D} \sim \text{gp}(\hat{f}_i, \hat{k}_i)$, where \hat{f}_i and \hat{k}_i are the posterior mean and kernel, respectively. The overall posterior process is $\mathbf{f} \mid \mathcal{D} \sim \text{gp}(\hat{\mathbf{f}}, \hat{\otimes}_{i=1}^m \hat{k}_i)$, where \otimes stands for the tensor product and $\hat{\mathbf{f}} = (\hat{f}_1, \hat{f}_2, \dots, \hat{f}_m)$. Quite a few works (see [ARL12] for an overview) have been devoted to model cross-correlations among GPs, e.g., multi-task GP [BCW07] and dependent GP [BF04]. In the following discussions, we shall always denote by \mathbf{y} the objective point $\mathbf{f}(\mathbf{x})$, namely $\mathbf{y} \mid \mathcal{D} \sim \mathcal{N}(\hat{\mathbf{f}}(\mathbf{x}), \text{diag}(\hat{\mathbf{s}}^2(\mathbf{x})))$, where $\hat{\mathbf{s}}^2(\mathbf{x}) = (\hat{k}_1(\mathbf{x}, \mathbf{x}), \dots, \hat{k}_m(\mathbf{x}, \mathbf{x}))$.

²It is possible to specify a prior mean function to the process. For brevity, we omit it from our discussion.

Several concepts of generalizing the expected improvement used in single objective Bayesian optimization are proposed in the relevant literature. An attempt to provide a comprehensive overview of earlier proposals was made in [WED⁺10]. The main directions are the use of the hypervolume indicator, as discussed in this paper, and the use of single objective scalarization functions. Noteworthy is the approach suggested by Keane [Kea06], where the center of gravity of the predictive probability distribution restricted to the non-dominated subspace is computed using similar probability distributions as discussed in this paper but not considering the hypervolume indicator. The survey by Wagner et al. [WED⁺10] revealed that hypervolume indicator based improvements have some favorable properties upon other proposals in terms of monotonicity properties, in the sense that larger expected value vectors, as well as larger variance vectors are rewarded, supporting exploitation and, respectively, exploration in infill criteria of Bayesian optimization.

Hypervolume Improvement Being a well-studied performance indicator for MOPs, the hypervolume (HV) indicator of a set $Y \subseteq \mathbb{R}^m$ is defined as the Lebesgue measure λ_m of the set that is dominated by Y and restricted by a reference point $\mathbf{r} \in \mathbb{R}^m$ (see Fig. 1 for an illustration), i.e., $\text{HV}(Y, \mathbf{r}) = \lambda_m(\cup_{\mathbf{y} \in Y} [\mathbf{y}, \mathbf{r}])$. The hypervolume indicator is often taken as a performance metric for comparing the empirical performance of MOAs [ZTL⁺03] or used in the indicator-based optimization algorithms [BNE07]. The contribution of a single objective vector \mathbf{y} to Y can be quantified by the well-known *hypervolume improvement* (HVI):

$$\Delta^+ : \mathbb{R}^m \rightarrow \mathbb{R}_{\geq 0}, \quad \Delta^+(\mathbf{y}; Y, \mathbf{r}) = \text{HV}(Y \cup \{\mathbf{y}\}, \mathbf{r}) - \text{HV}(Y, \mathbf{r}), \quad (1)$$

which serves as the base for various acquisition functions in the multi-objective Bayesian optimization algorithms. Note that the “plus” superscript on Δ^+ is to indicate its co-domain is non-negative, which helps distinguish itself from its generalization - “negative hypervolume improvement” (see Sec. 3). HVI has been playing a dominant role in generalizing the acquisition function for MOPs. We briefly recap some widely-used multi-objective acquisition functions.

Probability of Improvement (PoI) [Stu88] is generalized to multi-objective optimization in [EGN06, Kea06], which is defined as the probability that \mathbf{y} lies in the non-dominated set of \mathcal{P} , i.e., $\text{PoI}(\mathbf{x}; \mathcal{P}) = \mathbb{E}\{\mathbb{1}_{\text{ndom}(\mathcal{P})}(\mathbf{y}) \mid \mathcal{D}, \mathbf{x}\}$, where $\mathbb{1}$ is the characteristic function. Since PoI does not require the user to determine a reference point a priori, it is commonly applied in many scenarios. Based on PoI, the ε -*Probability of Improvement* (ε -PoI) is devised recently [EYD20], which only consider objective points that have at least a “distance” of ε to \mathcal{P} : $\forall \varepsilon \in \mathbb{R}_{\geq 0}$, $\varepsilon\text{-PoI}(\mathbf{x}; \mathcal{P}, \varepsilon) = \mathbb{E}\{\mathbb{1}_{\text{ndom}(\mathcal{P})}(\mathbf{y} + \varepsilon \mathbf{1}_m) \mid \mathcal{D}, \mathbf{x}\}$, where $\mathbf{1}_m$ is a m -dimensional vector consisting of 1’s.

Alternatively, *naïve Upper Confidence Bound* (naïve-UCB) [SKK⁺10, EYD20] considers the variability of the hypervolume improvement, which is defined as the HVI of an upper³ confidence bound of \mathbf{y} , i.e., $\hat{\mathbf{f}}(\mathbf{x}) - \omega \hat{\mathbf{s}}(\mathbf{x})$, where $\omega \in \mathbb{R}_{\geq 0}$ is the confidence level: $\text{naïve-UCB}(\mathbf{x}; \mathcal{P}, \mathbf{r}, \omega) = \Delta^+(\hat{\mathbf{f}}(\mathbf{x}) - \omega \hat{\mathbf{s}}(\mathbf{x}); \mathcal{P}, \mathbf{r})$. Hereinafter, when the Pareto approximation set \mathcal{P} and the reference point \mathbf{r} are clear from the context, we shall simply denote the HVI of an objective point \mathbf{y} as $\Delta^+(\mathbf{y})$.

3 The Distribution of Hypervolume Improvement

Consider a decision point $\mathbf{x} \in \mathcal{X}$ and its objective point \mathbf{y} . We depict some examples of its hypervolume improvement $\Delta^+(\mathbf{y})$ for $m = 2$ in Fig. 1. It can be observed from the figure that the exact expression of $\Delta^+(\mathbf{y})$ depends on the subset of \mathcal{P} that it dominates, indicating the expression of $\Delta^+(\mathbf{y})$ varies across realizations of \mathbf{y} , which brings the difficult of deriving the distribution function. Noticing that HVI on \mathbb{R}^m is actually a piecewise-defined function, it suffices to firstly identify the set on which the restriction of Δ^+ is not piecewise and then derive the conditional distribution function of HVI on such a set. As the first step, we provide a characterization of such a set.

Lemma 1. *Given a Pareto approximation set $\mathcal{P} \subset \mathbb{R}^m$ and a compact and connected set $S \subset \mathbb{R}^m$ that dominates \mathcal{P} . If every point in S dominates the same subset of \mathcal{P} , then the restriction $\Delta^+|_S$ is not a piecewise function and continuous.*

Proof. Let $U = \{\mathbf{p} \in \mathcal{P} : \forall \mathbf{s} \in S (\mathbf{s} \prec \mathbf{p})\}$. Based on the assumption that every point in S dominates the same subset U of \mathcal{P} , we could reformulate for every point \mathbf{s} , its hypervolume improvement, namely $\Delta^+(\mathbf{s}) = \text{HV}((\mathcal{P} \setminus U) \cup \{\mathbf{s}\}) - \text{HV}(\mathcal{P})$. Since $\mathcal{P} \setminus U$ and $\{\mathbf{s}\}$ are mutually non-dominated by construction, $\text{HV}((\mathcal{P} \setminus U) \cup \{\mathbf{s}\})$ is not piecewise-defined and continuous. \square

Apparently, the largest sets satisfying Lemma 1 are the “cells” formed by all the $m - 1$ dimensional linear sub-manifolds that pass through points in \mathcal{P} and are perpendicular to an axis of \mathbb{R}^m . For the bi-objective case ($m = 2$), we show an example of those cells in Fig. 1. In the paper, we focus on the bi-objective case and we use the following notations for convenience: $\forall \mathbf{x} \in \mathcal{X}$, $\mu_1 = \hat{f}_1(\mathbf{x})$, $\mu_2 = \hat{f}_2(\mathbf{x})$, and $\sigma_1^2 = \hat{k}_1(\mathbf{x}, \mathbf{x})$, $\sigma_2^2 = \hat{k}_2(\mathbf{x}, \mathbf{x})$.

³More precisely, it is a lower confidence bound when dealing with a minimization problem.

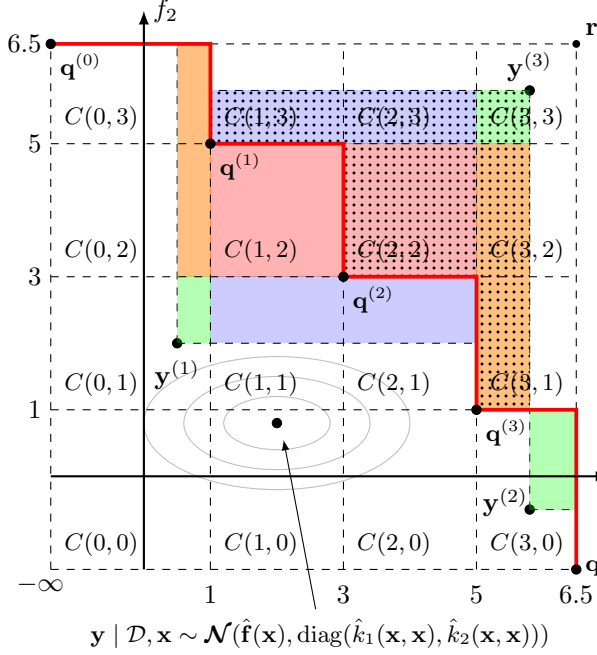


Figure 1: For a two-dimensional objective space, we picture the augmented Pareto approximation set $\tilde{\mathcal{P}}$ by the black dots ($\mathbf{q}^{(0)}, \dots, \mathbf{q}^{(4)}$) and the predictive distribution of $\mathbf{y} = \mathbf{f}(\mathbf{x})$ by the ellipsoids (in light gray). The hypervolume improvement of three realizations $\mathbf{y}^{(1)}, \mathbf{y}^{(2)}$, and $\mathbf{y}^{(3)}$ are depicted in shaded area, whose calculation depends on the points it dominates in $\tilde{\mathcal{P}}$. The objective space $[-\infty, \mathbf{r}]$ is decomposed into rectangular cells (e.g., $C(1, 0)$). When restricting the random point \mathbf{y} to a cell, its hypervolume can always be expressed in four parts, e.g., $\Delta^+(\mathbf{y}^{(1)})|_{C(0,1)} = \lambda_m(\text{blue}) + \lambda_m(\text{orange}) + \lambda_m(\text{red}) + \lambda_m(\text{green})$ (λ_m is the Lebesgue measure in \mathbb{R}^m). When a point is dominated by $\tilde{\mathcal{P}}$, its negative hypervolume improvement can be written similarly, e.g., $\Delta^-(\mathbf{y}^{(3)})|_{C(3,3)} = -\lambda_m(\text{blue}) - \lambda_m(\text{orange}) - \lambda_m(\text{red}) - \lambda_m(\text{green})$.

Cell decomposition of the objective space Assume a reference point $\mathbf{r} \in \mathbb{R}^m$, which is required to be dominated by every point in \mathcal{P} . We augment the Pareto approximation set $\tilde{\mathcal{P}} = \mathcal{P} \cup \{(\mathbf{r}_1, -\infty), (-\infty, \mathbf{r}_2)\}$ and index the points in $\tilde{\mathcal{P}}$ according to the increasing order of their first objective values, i.e., $\mathbf{q}^{(0)}, \mathbf{q}^{(1)}, \dots, \mathbf{q}^{(n+1)}$ where $q_1^{(0)} < q_1^{(1)} < \dots < q_1^{(n+1)}$. Let $C(i, j)$ ($i \in [0..n], j \in [0..n]$) represent the boxes formed by axis-parallel lines that pass through the points in $\tilde{\mathcal{P}}$, where the cells are indexed according to the increasing order of each component of its bottom-left point (see Fig. 1): $C(i, j) = [\mathbf{l}^{(i,j)}, \mathbf{u}^{(i,j)}]$, where left lower and the right upper points, $\mathbf{l}^{(i,j)}$ and $\mathbf{u}^{(i,j)}$ can be determined from $\tilde{\mathcal{P}}$:

$$\mathbf{l}^{(i,j)} = (q_1^{(i)}, q_2^{(n+1-j)})^\top, \mathbf{u}^{(i,j)} = (q_1^{(i+1)}, q_2^{(n-j)})^\top. \quad (2)$$

The entire objective space $[-\infty, \mathbf{r}]$ is decomposed into $(n+1)^2$ cells, i.e., $[-\infty, \mathbf{r}] = \cup_{i,j \in [0..n]} C(i, j)$. Note that, for $i+j \leq n$, the union of the cells $C(i, j)$ represents the set dominating $\tilde{\mathcal{P}}$ while $i+j > n$, it indicates the set dominated by $\tilde{\mathcal{P}}$.

Generalized hypervolume improvement When the random variable \mathbf{y} lies in the dominated set of \mathcal{P} (i.e., in cells $C(i, j)$ with $i+j > n$), the hypervolume improvement $\Delta(\mathbf{y})$ is by definition (Eq. 1) zero. However, such a behavior is not preferable whenever (1) in the global search scenario, the target MOP exhibits local Pareto optima, for which we do wish to assign a nonzero hypervolume improvement value to local Pareto fronts, and (2) when \mathbf{y} has a small probability to dominate \mathcal{P} (which can happen if the mean of \mathbf{y} lies in the dominated set and its variance is small), the probability density of $\Delta(\mathbf{y})$ will become essentially a Dirac delta function. In this case, if we were to pick the best decision point among several candidates at which the predictive distribution of \mathbf{y} satisfying scenario (2), the hypervolume improvement would be provide much useful information. In this regard, we extend the co-domain of HVI to \mathbb{R} by defining the *negative hypervolume improvement* $\Delta^-(\mathbf{y}) = -\lambda_m(\text{dom}(\tilde{\mathcal{P}}) \cap \text{ndom}(\{\mathbf{y}\}))$, where the negative hypervolume improvement Δ^- is defined as the Lebesgue measure of intersection of the dominated space w.r.t. $\tilde{\mathcal{P}}$ and the non-dominated space w.r.t. \mathbf{y} (see Fig. 1 for an illustration), which penalizes the objective point \mathbf{y} when it moves away from $\tilde{\mathcal{P}}$. Finally, the *generalized hypervolume improvement* is:

$$\Delta(\mathbf{y}) = \mathbb{1}_{\text{ndom}(\tilde{\mathcal{P}})}(\mathbf{y})\Delta^+(\mathbf{y}) + \mathbb{1}_{\text{dom}(\tilde{\mathcal{P}})}(\mathbf{y})\Delta^-(\mathbf{y}). \quad (3)$$

Taking the cell decomposition and the generalized hypervolume improvement into account, we can express the distribution functions of HVI by marginalizing the conditional distributions over cells: $F_{\Delta(\mathbf{y})|\mathcal{D}}(\delta) = \sum_{i,j \in [0..n]} F_{\Delta(\mathbf{y})|C(i,j)}(\delta) \Pr(\mathbf{y} \in C(i, j) \mid \mathcal{D}, \mathbf{x})$, where $F \in \{\text{PDF}, \text{CDF}\}$ and $\Pr(\mathbf{y} \in C(i, j) \mid \mathcal{D}) = \prod_{k \in \{1,2\}} [\Phi_{\mu_k, \sigma_k}(u_k^{(i,j)}) - \Phi_{\mu_k, \sigma_k}(l_k^{(i,j)})]$. In the above expression, the first term within the summation is condi-

tional distribution of Δ restricted to a cell and the second term is simply the probability of \mathbf{y} being in a cell $C(i, j)$, which is can be calculated directly with cell's definition and the distribution of \mathbf{y} .

Conditional probability density function When restricting \mathbf{y} in a cell $C(i, j)$, we can always express its hypervolume improvement in four parts (cf. Fig. 1 and Lemma 1). For the cells in the non-dominated space, i.e., $i + j \leq n$, the hypervolume improvement reads:

$$\begin{aligned} \Delta^+(\mathbf{y})|_{C(i,j)} &= \lambda_m(\text{green}) + \lambda_m(\text{blue}) + \lambda_m(\text{red}) + \lambda_m(\text{pink}) \\ &= \underbrace{(q_1^{(n+1-j)} - y_1)}_{y'_1} \underbrace{(q_2^{(i)} - y_2)}_{y'_2} + \underbrace{\Delta^+(\mathbf{u}^{(i,j)}) - (q_1^{(n+1-j)} - u_1^{(i,j)})(q_2^{(i)} - u_2^{(i,j)})}_{\gamma^{(i,j)}}, \end{aligned}$$

where $y'_1 \sim \mathcal{N}(q_1^{(n+1-j)} - \mu_1, \sigma_1^2)$ and $y'_2 \sim \mathcal{N}(q_2^{(i)} - \mu_2, \sigma_2^2)$ are Gaussian random variables truncated to $[L_1, U_1] := [q_1^{(n+1-j)} - u_1^{(i,j)}, q_1^{(n+1-j)} - l_1^{(i,j)}]$ and $[L_2, U_2] := [q_2^{(i)} - u_2^{(i,j)}, q_2^{(i)} - l_2^{(i,j)}]$, respectively. Let $\mu'_1 = q_1^{(n+1-j)} - \mu_1$, $\mu'_2 = q_2^{(i)} - \mu_2$, $D_1 = (\Phi_{\mu'_1, \sigma_1}(U_1) - \Phi_{\mu'_1, \sigma_1}(L_1))^{-1}$, and $D_2 = (\Phi_{\mu'_2, \sigma_2}(U_2) - \Phi_{\mu'_2, \sigma_2}(L_2))^{-1}$. Based on the result of distribution of the product of Gaussian [GLS04], we proceed with the conditional distribution of $\Delta^+(\mathbf{y})$: $\forall \delta \in [\Delta^+(\mathbf{u}^{(i,j)}), \Delta^+(\mathbf{l}^{(i,j)})]$, let $p := \delta - \gamma^{(i,j)} \in [L_1 L_2, U_1 U_2]$, we have

$$\text{PDF}_{\Delta^+(\mathbf{y})|_{C(i,j)}}(\delta) = \text{PDF}_{y'_1 y'_2|_{C(i,j)}}(\delta - \gamma^{(i,j)}) = D_1 D_2 \int_{\alpha(p)}^{\beta(p)} \phi_{\mu'_1, \sigma_1}(\zeta) \phi_{\mu'_2, \sigma_2}\left(\frac{p}{\zeta}\right) \frac{d\zeta}{\zeta}, \quad (4)$$

where the integral bounds are determined as follows. If $L_1 U_2 < U_1 L_2$, we define:

$$[\alpha(p), \beta(p)] = \begin{cases} [L_1, p/L_2], & L_1 L_2 \leq p < L_1 U_2 \\ [p/U_2, p/L_2], & L_1 U_2 \leq p < U_1 L_2 \\ [p/U_2, U_1], & U_1 L_2 \leq p \leq U_1 U_2 \end{cases} \quad (5)$$

When $L_1 U_2 > U_1 L_2$, it suffices to swap variables y'_1 and y'_2 and apply Eq. (5). For a cell in the dominated space, i.e., $C(i, j)$ with $i + j > n$, we can invert the coordinate system such that the computation on this cell can be treated in the same way as the non-dominated part, i.e., we set $[L_1^-, U_1^-] := [-U_1, -L_1]$, $[L_2^-, U_2^-] := [-U_2, -L_2]$, $\mu_1^- = -\mu'_1$, and $\mu_2^- = -\mu'_2$. Then, its conditional density can be computed with Eq. (4) as follows: $\forall \delta \in [\Delta^-(\mathbf{u}^{(i,j)}), \Delta^-(\mathbf{l}^{(i,j)})]$, $\text{PDF}_{\Delta^-(\mathbf{y})|_{C(i,j)}}(\delta) = \text{PDF}_{\Delta^+(\mathbf{y})|_{C(i,j)}}(-\delta)$, in which we substitute the constants (e.g., L_1) with the inverted ones (e.g., L_1^-).

Conditional cumulative distribution function Taking the conditional density function, the cumulative distribution of the hypervolume improvement can be derived for cells in $\text{ndom}(\tilde{\mathcal{P}})$:

$$\begin{aligned} \text{CDF}_{\Delta^+(\mathbf{y})|_{C(i,j)}}(\delta) &= \int_{L_1 L_2}^p \text{PDF}_{y'_1 y'_2|_{C(i,j)}}(z) dz \quad (p := \delta - \gamma^{(i,j)}) \\ &= \Phi_{\mu'_2, \sigma_2}(U_2) [\Phi_{\mu'_1, \sigma_1}(\alpha(p)) - \Phi_{\mu'_1, \sigma_1}(L_1)] + \Phi_{\mu'_2, \sigma_2}(L_2) [\Phi_{\mu'_1, \sigma_1}(L_1) - \Phi_{\mu'_1, \sigma_1}(\beta(p))] \\ &\quad + \int_{\alpha(p)}^{\beta(p)} \phi_{\mu'_1, \sigma_1}(\zeta) \Phi_{\mu'_2, \sigma_2}\left(\frac{p}{\zeta}\right) d\zeta. \end{aligned} \quad (6)$$

For cells in the dominated space ($C(i, j)$ with $i + j > n$), its cumulative distribution function is $\text{CDF}_{\Delta^-(\mathbf{y})|_{C(i,j)}}(\delta) = 1 - \text{CDF}_{\Delta^+(\mathbf{y})|_{C(i,j)}}(\delta)$.

Numerical computation We use the numerical integration⁴ to compute the distribution function in each cell and set the absolute error of the integration to 10^{-8} . Loosely speaking, the time complexity of the PDF and CDF of HVI is quadratic for bi-objective problems since we have to iterate over all cells. To reduce the time complexity, we propose to prune the cell on which the probability mass of \mathbf{y} is sufficiently small: only the cells that locates between $\mu - 3\sigma$ and $\mu + 3\sigma$ are used for the computation. In the left plot of Fig 2, we have illustrated an example of the CDF of HVI computed from both the exact distribution and the Monte-Carlo (MC) method. It is necessary to compare the computational cost of the exact distribution to that of the MC method to approximate the the cumulative distribution function. Generally, for achieving an accuracy of ε , the numerical integration requires $O(\varepsilon^{-1})$ [Nov14], resulting in an overall complexity of $O(\varepsilon^{-1}(n+1)^2)$ for the exact method. In contrast, the MC method requires sampling $O(\varepsilon^{-2})$

⁴We employed the 21-point Gauss-Kronrod quadrature method with maximally 50 sub-intervals.

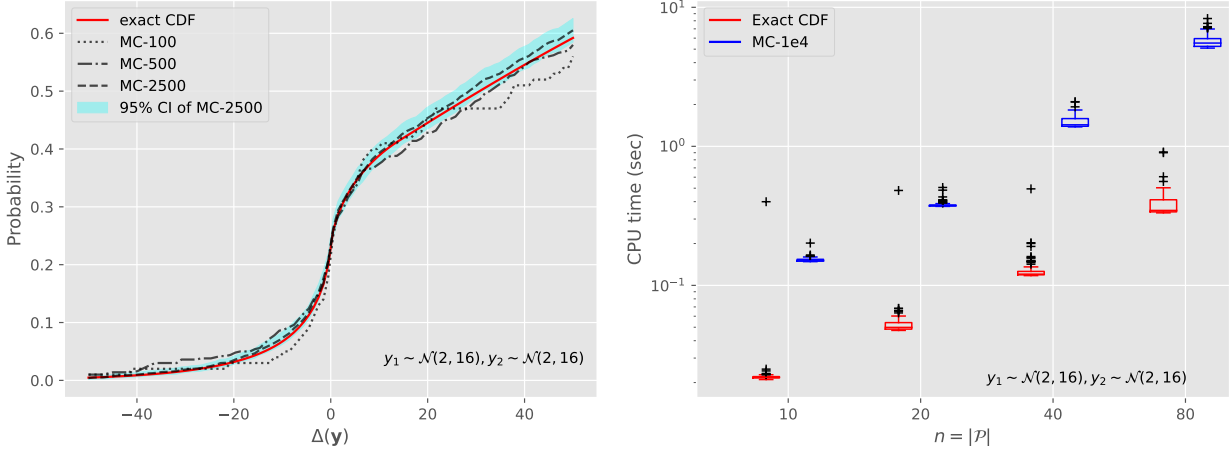


Figure 2: **Left:** For the Pareto front in Fig. 1, we show the CDF of \mathbf{y} computed from the exact and MC methods (using 100, 500, and 2500 samples). **Right:** The CPU time for the exact and the MC method (with 10^4 sample points) w.r.t. an increasing number of points of \mathcal{P} .

realizations of \mathbf{y} and calculating the hypervolume improvement thereof⁵, giving rise to a complexity of $O(\varepsilon^{-2} n \ln n)$. Also, in the right plot of Fig. 2, we compare the CPU time of the exact the MC computation when varying the number of points in the Pareto front, which shows that under a comparable numerical accuracy, the CPU time consumed by the exact computation is roughly one order of magnitude lower than that of the MC method, for a wide range of the cardinality of \mathcal{P} .

4 Acquisition functions based on the distribution of HVI

Upper Confidence Bound (UCB) The naïve-UCB only consider the variability of \mathbf{y} rather than directly bounding the uncertainty of the HVI resulted from \mathbf{y} . With the exact distribution functions of HVI, we can remedy this shortcoming by using the inverse of the CDF of HVI, i.e., $\forall \omega \in \mathbb{R}_{\geq 0}$, $\text{UCB}(\mathbf{x}; \mathcal{P}, \mathbf{r}, \omega) = \text{CDF}_{\Delta(\mathbf{y})|\mathcal{D}, \mathbf{x}}^{-1}(\omega)$, where $\Delta(\mathbf{y})$ lies in the one-sided confidence interval $[-\infty, \text{UCB}(\mathbf{x}; \mathcal{P}, \mathbf{r}, \omega)]$ with probability ω . Note that, it is not straightforward to derive the inverse of $\text{CDF}_{\Delta(\mathbf{y})|\mathcal{D}, \mathbf{x}}$ and hence we compute it numerically using Newton’s method (where $\text{d CDF}_{\Delta(\mathbf{y})|\mathcal{D}, \mathbf{x}} = \text{PDF}_{\Delta(\mathbf{y})|\mathcal{D}, \mathbf{x}} d\delta$).

ε -Probability of Hypervolume Improvement (ε -PoHVI) Similarly, ε -PoI controls the smallest “distance” from the objective point \mathbf{y} to \mathcal{P} , which is not directly related to the minimal hypervolume improvement of \mathbf{y} . The distribution of the HVI can help solve this drawback by considering the probability of making at least $\varepsilon\%$ improvement to the hypervolume of the Pareto approximation set:

$$\varepsilon\text{-PoHVI}(\mathbf{x}; \mathcal{P}, \mathbf{r}, \varepsilon) = 1 - \text{CDF}_{\Delta(\mathbf{y})|\mathcal{D}, \mathbf{x}}(\varepsilon \text{HV}(\mathcal{P}, \mathbf{r})). \quad (7)$$

Notably, although ε -PoHVI is defined in a more sensible way than ε -PoI, it requires the user to specify a reference point, which can be less convenient compared to ε -PoI in practice.

Experimental setup We investigate the empirical performance of the proposed acquisition functions on the well-known bi-objective ZDT problems [ZDT⁺00], in which we compare UCB and ε -PoHVI to naïve-UCB and ε -PoI with 15 independent runs on each problem. Among ZDT problems, we selected ZDT1 – 4 and 6 (since ZDT5 is discrete optimization problem), where the decision space $\mathcal{X} = [0, 1]^{30}$ for ZDT1 – 3 and $\mathcal{X} = [0, 1]^{10}$ for ZDT4 and 6. We initialize a Bayesian optimization algorithm (see <https://github.com/wangronin/HVI-distribution> for our implementation of BO and acquisition functions) with 30 points for the initial DoE and a total budget of 200 function evaluations. In the objective space, we take the reference point $\mathbf{r} = [15, 15]$ as recommended in [ZDT⁺00] when computing the hypervolume. Notably, ZDT4 is a multi-modal problem containing many local efficient sets and hence is deemed relatively harder to solve. Also, the Pareto front of ZDT6 does not span the whole range of the reference space $[0, 15]^2$, which might bring extra challenges.

⁵It requires computing the hypervolume of the Pareto front approximation, which has a time complexity of $O(n \ln n)$ when $m = 2, 3$ [BFL⁺09].

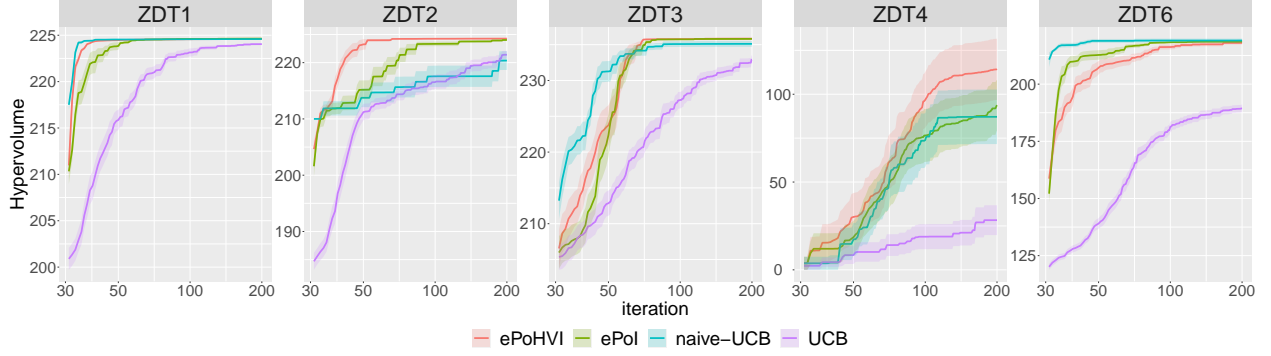


Figure 3: The mean hypervolume of the best-so-far Pareto approximation set \mathcal{P} plotted against the BO’s iteration. The shade area represents the 95% confidence interval of the mean, in which 15 independent runs are conducted for each acquisition function.

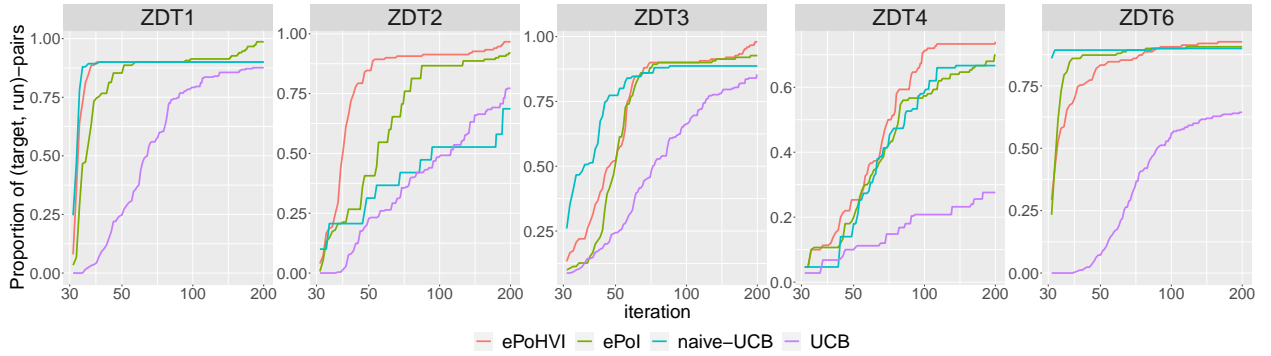


Figure 4: Empirical Cumulative Distribution Function (ECDF) of the iterations required by each acquisition function to hit a target hypervolume value. Moreover, the ECDF curves are aggregated over ten targets on each problem, which are log-evenly spaced between the minimal and maximal measured hypervolume values across all acquisition functions.

For ε -PoI, we set its hyperparameter ε to a fixed value of 0.05, while for ε -PoHVI, we use the following schedule for its hyperparameter $\varepsilon = 0.05 \times \exp(-0.02t)$, where t stands for the iteration counter of BO after the initial DoE. The usage of a decreasing schedule for ε -PoHVI is because the minimally required improvement $\varepsilon \text{ HV}(\mathcal{P}, \mathbf{r})$ depends on the hypervolume of the current Pareto approximation set, which will grow quickly and hence leads a very greedy behavior if ε is set to a constant. To counter such a greedy behavior, we decrease the ε value exponentially over time. In addition, we use the following monotonic schedules $\omega = \sqrt{t/\log t}$ and $\omega = \Phi(0.55\sqrt{\log 25t})$ for naïve-UCB and UCB, respectively, which are manually set up to maintain roughly the same confidence level for naïve-UCB and UCB.

Experimental results In Fig. 3, we show the mean convergence of the BO algorithm (in terms of the hypervolume of the best-so-far \mathcal{P}) when equipped with different bi-objective acquisition functions. It is evident that ε -PoHVI, which utilizes the distribution of HVI, exhibits either a faster (on ZDT2 and 4) or equal (on ZDT1 and 3) convergence speed compared to that of ε -PoI or naïve-UCB. Particularly, on ZDT4, which contains many local efficient sets, ε -PoHVI surpasses other acquisition functions substantially, suggesting that it is less prone to local stagnation and is more beneficial on multi-modal problems. On the contrary, on ZDT6, both ε -PoI and naïve-UCB outperform the ε -PoHVI function. A probable explanation is: The Pareto front of this problem spans ca. $[0.28, 1]$ on the first objective and ca. $[0, 0.92]$ on the second objective. Therefore, when using a reference point of $[15, 15]$, the region beyond the extreme point: $[0, 0.28] \times [0.92, 15]$, which has no pre-image in the decision space, will induce a considerable hypervolume improvement. Compared to ε -PoI (free of the reference point) or naïve-UCB (not heavily impacted by the reference point), the ε -PoHVI function is more inclined to suggest a candidate point beyond the extreme point when the reference point is set too big, thereby wasting more function evaluations in exploring an unreachable region in the objective space.

Moreover, we have observed that the other newly proposed acquisition function, UCB is always inferior to other alternatives across all problems, which might be caused by the sub-optimal schedule/setting of its hyperparameter ω . We shall investigate the behavior of UCB and the optimal setting thereof in the future. In Fig. 4, we illustrate the empirical cumulative distribution function (ECDF) of the running time (number of the iterations) taken by the BO to

reach a set of target hypervolume values, i.e., $\text{ECDF}(t) = (R|\mathcal{V}|)^{-1} \sum_{v \in \mathcal{V}} \sum_{i=1}^R \mathbb{1}_{(-\infty, t]}(T(v, i))$, where \mathcal{V} is a set of target hypervolume values, R is the number of independent runs, and $T(v, i)$ represents the number of iterations that BO takes to hit target $v \in \mathcal{V}$ in run $i \in [1..R]$. Specifically, we use ten target values on each problem, which are log-evenly spaced between the minimal and maximal measured hypervolume across all acquisition functions. In this manner, such an ECDF considers the distribution of running time for solving easy as well as hard target values, therefore providing a quantification of anytime performance. In terms of this ECDF measure, ε -PoHVI shows better performance on all problems except ZDT1, where the advantage is only realized for a relatively large running time on ZDT3 and ZDT6.

5 Conclusions and Future Works

In this work, we have provided the exact expression of the distribution functions of the hypervolume improvement (HVI) in bi-objective Bayesian optimization. Assuming a bivariate Gaussian distribution of an objective point (e.g., rising from the Gaussian process model of objective functions), we derive the distribution functions of the HVI brought by this point by partitioning the objective space into cells, on which we can provide a closed-form expression for the conditional distribution of HVI. We compared the numerical computation of the exact expression to that of a Monte-Carlo (MC) approach, showing that the exact method is faster and more accurate than the MC computation.

Also, we propose two novel multi-objective acquisition functions based on the newly-derived distribution function of HVI, i.e., Upper Confidence Bound (UCB) and ε -Probability of Hypervolume Improvement (ε -PoHVI), which are validated and compared to the state-of-the-art acquisition functions on the well-known ZDT benchmark problems. The experimental result shows that ε -PoHVI is superior to other acquisition functions on multi-modal problems, whereas UCB is constantly outperformed across all problems.

In the future, we need to perform an in-depth study of the behaviour of the UCB function to figure out the reason behind its poor performance on ZDT problems. More importantly, we plan to extend the exact distribution function to objective spaces with higher dimensions.

References

- [ARL12] Mauricio A. Álvarez, Lorenzo Rosasco, and Neil D. Lawrence. Kernels for Vector-Valued Functions: A Review. *Found. Trends Mach. Learn.*, 4(3):195–266, 2012.
- [BFL⁺09] Nicola Beume, Carlos M. Fonseca, Manuel López-Ibáñez, Luís Paquete, and Jan Vahrenhold. On the Complexity of Computing the Hypervolume Indicator. *IEEE Trans. Evol. Comput.*, 13(5):1075–1082, 2009.
- [BNE07] Nicola Beume, Boris Naujoks, and Michael T. M. Emmerich. SMS-EMOA: multiobjective selection based on dominated hypervolume. *Eur. J. Oper. Res.*, 181(3):1653–1669, 2007.
- [BCW07] Edwin V. Bonilla, Kian Ming Adam Chai, and Christopher K. I. Williams. Multi-task Gaussian Process Prediction. In John C. Platt, Daphne Koller, Yoram Singer, and Sam T. Roweis, editors, *Advances in Neural Information Processing Systems 20, Proceedings of the Twenty-First Annual Conference on Neural Information Processing Systems, Vancouver, British Columbia, Canada, December 3-6, 2007*, pages 153–160. Curran Associates, Inc., 2007.
- [BF04] Phillip Boyle and Marcus R. Frean. Dependent Gaussian Processes. In *Advances in Neural Information Processing Systems 17 [Neural Information Processing Systems, NIPS 2004, December 13-18, 2004, Vancouver, British Columbia, Canada]*, pages 217–224, 2004.
- [DBB20] Samuel Daulton, Maximilian Balandat, and Eytan Bakshy. Differentiable Expected Hypervolume Improvement for Parallel Multi-Objective Bayesian Optimization. In Hugo Larochelle, Marc’Aurelio Ranzato, Raia Hadsell, Maria-Florina Balcan, and Hsuan-Tien Lin, editors, *Advances in Neural Information Processing Systems 33: Annual Conference on Neural Information Processing Systems 2020, NeurIPS 2020, December 6-12, 2020, virtual*, 2020.
- [DAP⁺02] Kalyanmoy Deb, Samir Agrawal, Amrit Pratap, and T. Meyarivan. A fast and elitist multiobjective genetic algorithm: NSGA-II. *IEEE Trans. Evol. Comput.*, 6(2):182–197, 2002.
- [EYD⁺16] Michael Emmerich, Kaifeng Yang, André H. Deutz, Hao Wang, and Carlos M. Fonseca. A Multicriteria Generalization of Bayesian Global Optimization. In Panos M. Pardalos, Anatoly Zhigljavsky, and Julius Zilinskas, editors, *Advances in Stochastic and Deterministic Global Optimization*, volume 107 of *Springer Optimization and Its Applications*, pages 229–242. Springer, 2016.

- [EGN06] Michael T. M. Emmerich, Kyriakos C. Giannakoglou, and Boris Naujoks. Single- and multiobjective evolutionary optimization assisted by Gaussian random field metamodels. *IEEE Trans. Evol. Comput.*, 10(4):421–439, 2006.
- [EYD20] Michael T. M. Emmerich, Kaifeng Yang, and André H. Deutz. Infill Criteria for Multiobjective Bayesian Optimization. In Thomas Bartz-Beielstein, Bogdan Filipic, Peter Korosec, and El-Ghazali Talbi, editors, *High-Performance Simulation-Based Optimization*, volume 833 of *Studies in Computational Intelligence*, pages 3–16. Springer, 2020.
- [Gen01] Marc G. Genton. Classes of Kernels for Machine Learning: A Statistics Perspective. *J. Mach. Learn. Res.*, 2:299–312, 2001.
- [GLS04] Andrew G. Glen, Lawrence M. Leemis, and John H. Drew. Computing the distribution of the product of two continuous random variables. *Comput. Stat. Data Anal.*, 44(3):451–464, 2004.
- [JSW98] Donald R. Jones, Matthias Schonlau, and William J. Welch. Efficient Global Optimization of Expensive Black-Box Functions. *Journal of Global Optimization*, 13(4):455–492, 1998.
- [Kea06] Andy J. Keane. Statistical improvement criteria for use in multiobjective design optimization. *American Institute of Aeronautics and Astronautics (AIAA) Journal*, 44(4):879–891, 2006.
- [Moc74] Jonas Mockus. On Bayesian Methods for Seeking the Extremum. In Guri I. Marchuk, editor, *Optimization Techniques, IFIP Technical Conference, Novosibirsk, USSR, July 1-7, 1974*, volume 27 of *Lecture Notes in Computer Science*, pages 400–404. Springer, 1974.
- [Nov14] Erich Novak. Some Results on the Complexity of Numerical Integration. In Ronald Cools and Dirk Nuyens, editors, *Monte Carlo and Quasi-Monte Carlo Methods, MCQMC 2014, Leuven, Belgium, April 2014*, volume 163 of *Springer Proceedings in Mathematics and Statistics*, pages 161–183. Springer, 2014.
- [RW06] Carl Edward Rasmussen and Christopher K. I. Williams. *Gaussian processes for machine learning*. Adaptive computation and machine learning. MIT Press, 2006.
- [SSW⁺16] Bobak Shahriari, Kevin Swersky, Ziyu Wang, Ryan P. Adams, and Nando de Freitas. Taking the Human Out of the Loop: A Review of Bayesian Optimization. *Proc. IEEE*, 104(1):148–175, 2016.
- [SKK⁺10] Niranjan Srinivas, Andreas Krause, Sham M. Kakade, and Matthias W. Seeger. Gaussian Process Optimization in the Bandit Setting: No Regret and Experimental Design. In Johannes Fürnkranz and Thorsten Joachims, editors, *Proceedings of the 27th International Conference on Machine Learning (ICML-10), June 21-24, 2010, Haifa, Israel*, pages 1015–1022. Omnipress, 2010.
- [Stu88] Bruce E. Stuckman. A global search method for optimizing nonlinear systems. *IEEE Trans. Syst. Man Cybern.*, 18(6):965–977, 1988.
- [YDY⁺16] Kaifeng Yang, André H. Deutz, Zhiwei Yang, Thomas Bäck, and Michael T. M. Emmerich. Truncated expected hypervolume improvement: Exact computation and application. In *IEEE Congress on Evolutionary Computation, CEC 2016, Vancouver, BC, Canada, July 24-29, 2016*, pages 4350–4357. IEEE, 2016.
- [YED⁺19a] Kaifeng Yang, Michael Emmerich, André H. Deutz, and Thomas Bäck. Efficient computation of expected hypervolume improvement using box decomposition algorithms. *J. Glob. Optim.*, 75(1):3–34, 2019.
- [YED⁺19b] Kaifeng Yang, Michael Emmerich, André H. Deutz, and Thomas Bäck. Multi-Objective Bayesian Global Optimization using expected hypervolume improvement gradient. *Swarm Evol. Comput.*, 44:945–956, 2019.
- [YLD⁺16] Kaifeng Yang, Longmei Li, André H. Deutz, Thomas Bäck, and Michael Emmerich. Preference-based multiobjective optimization using truncated expected hypervolume improvement. In *12th International Conference on Natural Computation, Fuzzy Systems and Knowledge Discovery, ICNC-FSKD 2016, Changsha, China, August 13-15, 2016*, pages 276–281. IEEE, 2016.
- [YPE⁺19] Kaifeng Yang, Pramudita Satria Palar, Michael Emmerich, Koji Shimoyama, and Thomas Bäck. A multi-point mechanism of expected hypervolume improvement for parallel multi-objective bayesian global optimization. In Anne Auger and Thomas Stützle, editors, *Proceedings of the Genetic and Evolutionary Computation Conference, GECCO 2019, Prague, Czech Republic, July 13-17, 2019*, pages 656–663. ACM, 2019.
- [ZDT⁺00] Eckart Zitzler, Kalyanmoy Deb, and Lothar Thiele. Comparison of multiobjective evolutionary algorithms: Empirical results. *Evol. Comput.*, 8(2):173–195, 2000.
- [ZTL⁺03] Eckart Zitzler, Lothar Thiele, Marco Laumanns, Carlos M. Fonseca, and Viviane Grunert da Fonseca. Performance assessment of multiobjective optimizers: an analysis and review. *IEEE Trans. Evol. Comput.*, 7(2):117–132, 2003.

- [WED⁺10] Tobias Wagner, Michael Emmerich, André Deutz, and Wolfgang Ponweiser. On expected-improvement criteria for model-based multi-objective optimization. In *International Conference on Parallel Problem Solving from Nature*, pages 718–727. Springer, 2010.